JOURNAL OF MATERIALS SCIENCE 28 (1993) 1814–1818

The relationship between ductility and material parameters for dual-phase steel

ZHONGHAO JIANG, ZHENZHONG GUAN,* JIANSHE LIAN
Department of Metal Materials Engineering, Jilin University of Technology, Changchun 130025, People's Republic of China
** Changchun Institute of Optics and Fine Mechanics, Chinese Academy of Sciences, Changchun 130025, People's Republic of China*

A modified Crussard–Jaoul analysis has been employed to describe the strain hardening behaviour (the $\ln(d\sigma/d\varepsilon)$ versus $\ln\sigma$ curves) of a 1020 dual-phase steel with quenching and quenching + tempering treatments and with different predeformations, which demonstrated that this dual-phase steel exhibits two stages of strain-hardening in the range of plastic deformation. An analysis of instability for dual-phase steel is also presented and the relationship between the maximum uniform strain and the material parameters is proposed, which shows good agreement with the experimental results for the present 1020 dual-phase steel and other dual-phase steels.

1. Introduction

Dual-phase steels whose microstructures consist of a ferrite matrix with particles of martensite have received a great deal of attention due to their useful combination of high strength and good ductility. These steels are characterized by a low initial flow stress and a high initial work-hardening rate. There have been numerous attempts to describe the stress–strain or strain-hardening behaviour of dual-phase steels [1–6]. The Crussard–Jaoul (C–J) analysis [9, 10] based on the Ludwik relation and a modified C–J analysis [11] based on the Swift relation have been applied to correlate the tensile stress–strain behaviours of dual-phase steels [5–8]. With the modified C–J analysis, it was shown that dual-phase steels deformed with two stages of strain hardening [5–8].

For plastic materials with a nearly constant strain-hardening exponent during plastic deformation, the relation between the instability strain (maximum uniform strain) and the strain-hardening exponent was established by the Considere analysis [11]. The relationships between the strain to fracture (or total elongation) and material parameters including both strain-hardening exponent and strain-rate sensitivity were derived by necking development analyses [12–15]. However, for materials with two stages of strain hardening, the relation between ductility and material parameters has not been established.

In the present study, the modified C–J analysis is applied to a 1020 dual-phase steel for describing its strain-hardening behaviour. A theoretical analysis of instability is then presented in order to derive the relationship between the ductility and the material parameters for dual-phase steel.

2. Experimental procedure

The material used in the experiments is a hot-rolled 1020 steel from hot-rolling bar of 18 mm diameter. Its chemical compositions in weight percentage are 0.2% C, 0.3%Si, 0.47%Mn, 0.02% P and 0.03% S. This material was first heated at 1100 °C for 4 h and air-cooled for obtaining a more uniform initial microstructure. Then it was normalized at 900 °C for 0.5 h and air-cooled, followed by drawing at room temperature with total reductions of area (RA) of 30, 50, and 70%. The dual-phase structure is obtained by heating the specimens in the intercritical temperature range (720–810 °C) for 20 min, then quenching in salt water (15% NaCl). A portion of the specimens were then tempered at 180 °C for 2 h. The volume fraction of martensite was measured on a Quantimet 970 image analyser. Tensile tests were carried out using an AG10T electronic tester at a crosshead speed of 1 mm min^{-1}. The dimensions of the cylindrical test specimen were 25 mm gauge length and 5 mm gauge section diameter. The results were analysed to obtain the true stress strain and $\ln(d\sigma/d\varepsilon)$ versus $\ln(\sigma)$ data and other mechanical properties. The strain-rate sensitivity $M = d(\ln\sigma)/d(\ln\varepsilon)$ was measured by the Backfen method [13].

3. Analysis

3.1. The modified C–J analysis

For the experimental analysis of the strain-hardening behaviour of dual-phase steel, the modified C–J analysis based on the Swift equation will be used. In this case, the Swift equation becomes

$$\varepsilon = k\sigma^m + \varepsilon_0 \quad (1)$$

0022–2461

The logarithmic form of Equation 1, differentiated with respect to ε, is

$$\ln(d\sigma/d\varepsilon) = (1 - m)\ln\sigma - \ln(km) \quad (2)$$

Fig. 1 shows several examples of the experimental $\ln(d\sigma/d\varepsilon)$ versus $\ln\sigma$ curves for 1020 dual-phase steel. According to Equation 2, the slope of these curves equals $1 - m$ and m reflects the strain-hardening of material. Fig. 1 reveals that the tested 1020 dual-phase steel exhibits two stages of strain hardening behaviour. The first stage has a low strain-hardening exponent, and the second stage has a high one. The m_1 and m_2 values for the composite with quenching and quenching + tempering procedures are listed in Table I, where m_1 is the strain-hardening exponent for the first stage and m_2 is that for the second stage. It was believed that the first stage was associated with

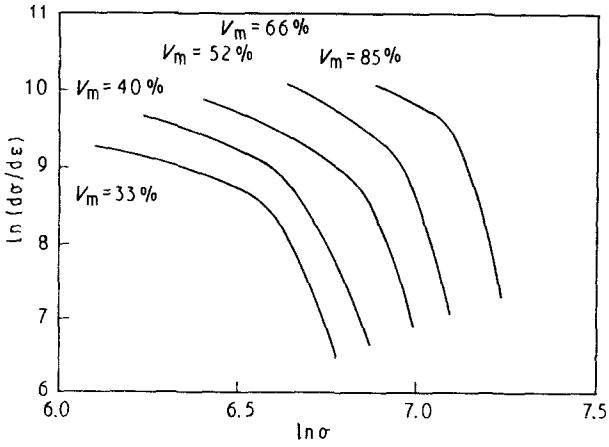

Figure 1 Several examples of experimental curves for 1020 dual-phase steel with quenching + tempering procedure and without predeformation.

TABLE I Data from modified C–J analysis and comparison of maximum uniform strain between calculated and experimental results for 1020 dual-phase steel

RA (%)	V_m (%)	m_1	m_2	σ_k/σ_u	ε_{01} ($\times 10^{-3}$)	ε_u^e	ε_u^c	M ($\times 10^{-3}$)
Quenching treatment								
0	33	2.80	15.0	0.881	− 4.87	0.113	0.105	6.13
0	40	2.83	15.5	0.894	− 4.46	0.105	0.111	8.12
0	52	3.08	16.4	0.881	− 4.89	0.095	0.089	8.29
0	66	3.20	18.5	0.886	− 5.51	0.086	0.076	8.89
0	85	3.45	21.5	0.897	− 6.80	0.071	0.063	9.45
30	33	2.44	14.2	0.883	− 6.82	0.110	0.122	
30	41	2.59	14.0	0.885	− 5.34	0.106	0.123	8.02
30	51	2.66	15.1	0.876	− 6.09	0.098	0.102	
30	65	2.96	16.1	0.879	− 7.48	0.090	0.088	8.30
30	85	3.15	20.6	0.887	− 7.15	0.074	0.064	
50	33	2.31	13.4	0.863	− 7.26	0.104	0.117	
50	41	2.33	13.6	0.862	− 6.60	0.106	0.114	7.53
50	51	2.81	13.6	0.860	− 5.81	0.099	0.104	
50	65	2.67	15.6	0.861	− 8.20	0.091	0.086	9.18
50	85	3.04	19.8	0.881	− 9.08	0.074	0.064	
70	33	2.24	14.6	0.875	− 9.42	0.099	0.113	
70	40	2.42	14.8	0.864	− 7.01	0.102	0.100	6.40
70	50	2.30	16.0	0.866	− 8.87	0.097	0.091	
70	65	2.57	16.8	0.873	− 9.90	0.088	0.083	7.70
70	85	2.82	21.4	0.899	− 9.99	0.073	0.068	
Quenching + tempering treatment								
0	33	3.70	10.5	0.829	− 4.26	0.122	0.115	8.72
0	40	3.76	11.6	0.868	− 4.53	0.110	0.117	9.00
0	52	3.68	12.3	0.856	− 4.74	0.092	0.105	10.21
0	66	4.20	14.4	0.868	− 4.37	0.085	0.089	11.75
0	85	4.24	17.7	0.882	− 6.22	0.071	0.070	12.61
30	33	4.26	9.0	0.838	− 5.78	0.136	0.131	
30	41	4.22	9.9	0.850	− 4.59	0.122	0.124	7.35
30	51	4.18	10.8	0.839	− 4.09	0.107	0.111	
30	65	4.64	12.3	0.846	− 5.17	0.092	0.093	9.80
30	85	4.70	17.1	0.886	− 5.41	0.075	0.073	
50	33	4.78	7.9	0.829	− 4.97	0.139	0.140	
50	41	4.74	9.0	0.847	− 4.68	0.123	0.129	8.30
50	51	5.17	9.6	0.829	− 3.39	0.109	0.116	
50	65	5.30	11.3	0.852	− 4.33	0.093	0.101	9.80
50	85	5.34	16.0	0.883	− 5.50	0.076	0.076	
70	33	5.33	8.9	0.860	− 5.05	0.129	0.127	
70	40	5.34	10.0	0.868	− 5.26	0.118	0.116	8.34
70	50	5.60	11.5	0.860	− 4.03	0.102	0.099	
70	65	5.60	13.6	0.886	− 3.73	0.089	0.090	10.83
70	85	5.83	17.5	0.896	− 5.18	0.075	0.069	

plastic deformation of ferrite phase while the martensite phase is in elasticity, and the second stage with plastic deformation of both ferrite and martensite phases [5–9]. Between the two stages, there is a transition strain (ε_k) which is determined as the strain where the slope of the $\ln(d\sigma/d\varepsilon)$ versus $\ln\sigma$ curves shows a maximum variation, and ε_k is considered to be the strain where both phases begin to deform plastically. Fig. 2 shows the variation of transition strain with volume fraction of martensite (V_m) for the composite with quenching and quenching + tempering treatments. For the composite with a smaller volume fraction of martensite, the first stage will continue to a larger strain, and for that with a larger volume fraction of martensite, martensite will begin to deform plastically early. Therefore, the transition strain (ε_k) decreases with increase of V_m.

3.2. Instability analysis

As it is shown in the above section that the stress–strain curves of the dual-phase steel exhibit two stages of strain-hardening, the Swift equation is applied to the two stages as follows:

$$\varepsilon = K_1\sigma^{m_1} + \varepsilon_{01} \quad \text{for stage 1, before } \varepsilon_k \quad (3)$$

$$\varepsilon = K_2\sigma^{m_2} + \varepsilon_{02} \quad \text{for stage 2, after } \varepsilon_k \quad (4)$$

where K_1, K_2, ε_{01} and ε_{02} are material constants and m_1, m_2 are the strain-hardening exponents for the two stages. The instability strain or maximum uniform strain ε_u can be written as

$$\varepsilon_u = \varepsilon_k + (\varepsilon_u - \varepsilon_k) \quad (5)$$

From Equation 4, the second term of the right hand-side of Equation 5 can be expressed as

$$\varepsilon_u - \varepsilon_k = K_2(\sigma_u^{m_2} - \sigma_k^{m_2}) \quad (6)$$

Differentiation of Equation 4 with respect to strain gives

$$1 = K_2 m_2 \sigma^{m_2-1}\frac{d\sigma}{d\varepsilon} \quad (7)$$

From the Considere instability criterion [16], we have

$$\frac{d\sigma}{d\varepsilon} = \sigma_u \quad (8)$$

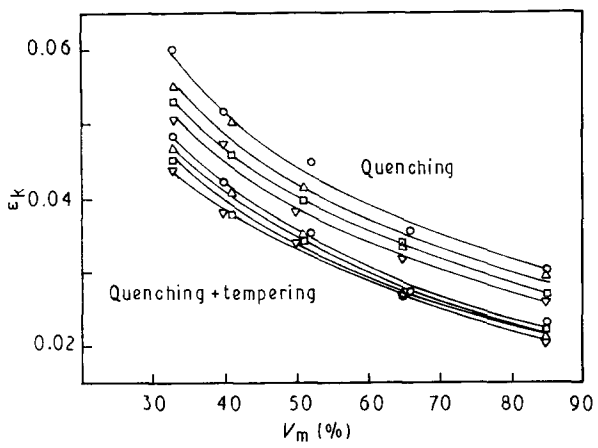

Figure 2 Variation of transition strain (ε_k) with volume fraction of martensite (V_m) for 1020 dual-phase steel. Reduction of area: (○) 0%, (△) 30%, (□) 50%, (▽) 70%.

Combination of Equation 7 with Equation 8 gives

$$K_2 = \frac{1}{m_2\sigma_u^{m_2}} \quad (9)$$

Introduction of Equation 9 into Equation 6 gives

$$\varepsilon_u = \varepsilon_k + \frac{1}{m_2}\left[1 - \left(\frac{\sigma_k}{\sigma_u}\right)^{m_2}\right] \quad (10)$$

At the transition strain ε_k, Equation 3 is expressed as

$$\varepsilon_k = K_1\sigma_k^{m_1} + \varepsilon_{01} \quad (11)$$

It is understood that at the transition strain the strain-hardening rates described by Equation 3 and Equation 4 are equal [15], i.e.

$$K_1 m_1 \sigma_k^{m_1-1} = K_2 m_2 \sigma_k^{m_2-1}$$

or

$$K_1 m_1 \sigma_k^{m_1} = K_2 m_2 \sigma_k^{m_2} \quad (12)$$

Introduction of Equation 9 into Equation 12 gives

$$K_1\sigma_k^{m_1} = \frac{1}{m_1}\left(\frac{\sigma_k}{\sigma_u}\right)^{m_2} \quad (13)$$

From Equations 10, 11 and 13 one has

$$\varepsilon_u = \varepsilon_{01} + \frac{1}{m_2} + \left(\frac{1}{m_1} - \frac{1}{m_2}\right)\left(\frac{\sigma_k}{\sigma_u}\right)^{m_2} \quad (14)$$

This is the relationship that relates the instability strain (maximum uniform strain) to the material parameters including the strain-hardening exponents for two stages, m_1 and m_2, the ratio of the stress at transition strain (σ_k) to that at maximum load (σ_u) and the constant ε_{01}.

4. Comparison with experiments

The experimental m_1, m_2, ε_{01} and σ_k/σ_u values for 1020 dual-phase steel for all the experimental procedures are listed in Table I. The measured strain-rate sensitivity exponents for 1020 dual-phase steel for various experimental conditions are also given in Table I. Using the necessary data, the maximum uniform strains ε_u^c were calculated with Equation 14 and listed in Table I for comparison with the experimental values (ε_u^e). It is seen that very good agreement was obtained between the calculated and experimental values of maximum uniform strain. However, it is apparent that Equation 14 is not practical for us to study the effect of the strain-hardening exponents m_1 and m_2 on the maximum uniform strain (ε_u) due to the fact that there are many variables involved in this equation. Fortunately, it can be found from Table I that ε_{01} values and the ratio σ_k/σ_u for all cases vary in a small range (-0.004 to -0.01, and 0.83–0.90). This result, in fact, is not surprising. For dual-phase steel, the increase of strength with strain primarily occurs in the low-strain range because of the high strain-hardening rate. In the high-strain range the rate of the increase of strength becomes small due to the rapid decrease in strain-hardening rate. For the present dual-phase steel shown in Table I, though the strain ε_k is smaller than a half of ε_u for all cases, the

increase of strength before strain ε_k is far larger than that after ε_k. Because of the insensitivity of ε_{01} values and the ratio of σ_k/σ_u to material parameters and experimental conditions, they can be considered as an adjustable material constants. In this case, Equation 14 can be converted to the following form:

$$\varepsilon_u = \alpha + \frac{1}{m_2} + \left(\frac{1}{m_1} - \frac{1}{m_2}\right)\beta^{m_2} \quad (15)$$

where $\alpha = \varepsilon_{01}$ and $\beta = \sigma_k/\sigma_u$. Equation 15 gives a simple relationship between maximum uniform strain and the strain-hardening exponents for materials with two stages of strain hardening. Apparently, this equation is a hemiempirical relationship which depends on a suitable selection of α and β. If α and β are independent of the levels of strength and ductility, ε_u is a function of only m_1 and m_2. Fig. 3 shows this relationship, in which α and β were taken as -0.005 and 0.87, respectively. These two values are the average values of ε_{01} and σ_k/σ_u for all the specimens of the present dual-phase steel. It is seen from Fig. 3 that the strain-hardening exponent for the second stage (m_2) exhibits a stronger influence on ε_u than m_1 does.

Fig. 4 presents a comparison between the theoretical maximum uniform strains calculated with Equation 15 (ε_u^c) with experimental values (ε_u^e) for the dual-phase steel examined in the present work and other dual-phase steels from previous studies [5, 18]. The same values of α and β (-0.005 and 0.87) were used for the other two dual-phase steels and their m_1 and m_2 values are shown in Table II. It is seen from Fig. 4 that good agreement between experiments and predicted results is obtained. Therefore, Equation 15 is suitable to describe the dependence of maximum uniform strain (instability strain) upon strain-hardening exponents for materials exhibiting two stages of strain-hardening.

4.1. Post-uniform strain

From the necking development analysis of Lian and Baudelet [13], the strain to fracture (ε_f) can be predicted by the relationship

$$\varepsilon_f = n - M\ln[1 - (1 - f)^{1/M}] \quad (16)$$

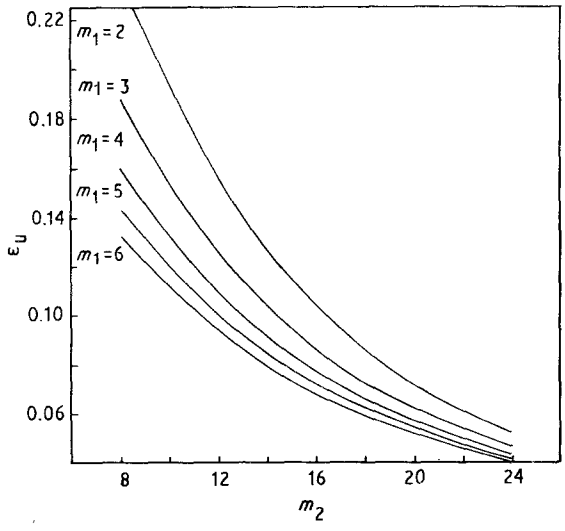

Figure 3 Influence of strain-hardening exponents on maximum uniform strain ε_u, calculated with Equation 15.

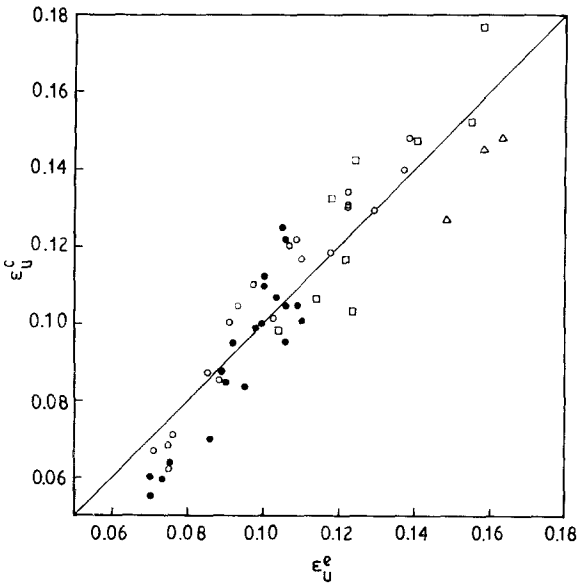

Figure 4 Comparison of maximum uniform strain between the experiments for 1020 dual-phase steel and two other dual-phase steels and the results predicted with Equation 15. (●) 1020 DPS Q, (○) 1020 DPS Q + T, (□) Fe–Mn–Si–C DPS[18], (△) Fe–0.1C DPS [5].

TABLE II Comparison of maximum uniform strain between theoretical calculations and experiments for dual-phase steels [5, 18]

m_1	m_2	ε_u^c	ε_u^e
Fe–Mn–Si–C DPS [17]			
5.23	8.56	0.119	0.133
6.58	10.57	0.124	0.103
6.11	9.51	0.122	0.116
5.60	11.58	0.104	0.098
4.16	6.87	0.159	0.177
5.42	7.14	0.154	0.152
4.64	8.19	0.141	0.147
4.67	8.39	0.123	0.144
6.85	10.00	0.114	0.106
Fe–0.1C DPS [5]			
6.28	8.36	0.148	0.127
4.96	8.01	0.158	0.147
4.98	7.77	0.163	0.148

where M and n are the strain-rate sensitivity and strain-hardening exponent of the material, respectively, and f is the initial geometrical imperfection of specimen. Based on the analyses of Nichols [11], Lian [12] and Semiatin and Jonas [14], another simpler relationship was derived:

$$\varepsilon_f = n + M\ln\left(\frac{1}{f}\right) \quad (17)$$

It was shown that Equation 16 can better predict the strain to fracture for many superplastic materials than Equation 17. However, it is believed that Equation 17 is able to predict the strain to fracture for general plastic materials. With the assumption that $\varepsilon_u = n$, the post-uniform strain expressed by Equation 17 is

$$\varepsilon_{pu} = \varepsilon_f - \varepsilon_u = M\ln\left(\frac{1}{f}\right) \quad (18)$$

Fig. 5 shows the comparison between the post-uniform elongation calculated with Equation 18 and the experimental values collected by Ghosh [17]. With the measured strain-rate sensitivity listed in Table I, the same comparison for 1020 dual-phase steel is shown in Fig. 6. Obviously, very good agreement has been obtained for several plastic materials (Fig. 5) and the present dual-phase steel (Fig. 6). Therefore, the simpler relationship of Equation 17 is useful to predict the strain to fracture for plastic materials. For dual-phase steel, with the maximum uniform strain expressed by Equation 15, the strain to fracture can be predicted by

$$\varepsilon_u = \alpha + \frac{1}{m_2} + \left(\frac{1}{m_1} - \frac{1}{m_2}\right)\beta^{m_1} + M\ln\left(\frac{1}{f}\right) \quad (19)$$

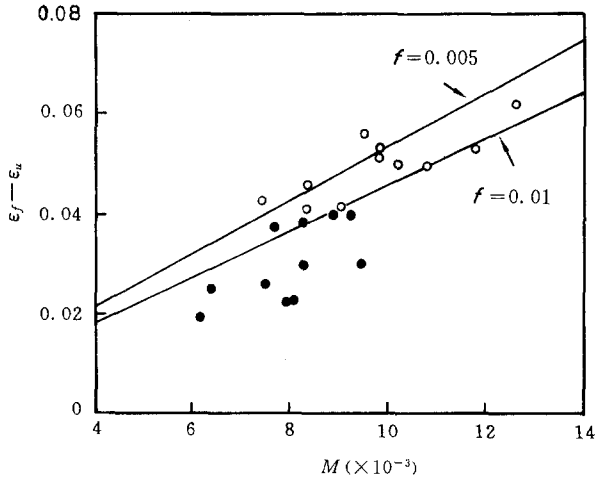

Figure 6 Relation between post-uniform strain and strain-rate sensitivity (M) for 1020 dual-phase steel. compared with theoretical calculation with Equation 18. (●) 1020 DPS Q, (○) 1020 DPS Q + T, (——) Equation 18.

5. Conclusion

1. A relationship between maximum uniform strain and material parameters has been proposed for plastic materials with two stages of strain-hardening behaviour, which shows very good agreement with experimental results for 1020 dual-phase steel and other dual-phase steels.

2. The relationship proposed by Nichols, Lian, and Semiatia and Jonas is suitable to predict the strain to fracture for many common plastic materials including dual-phase steel.

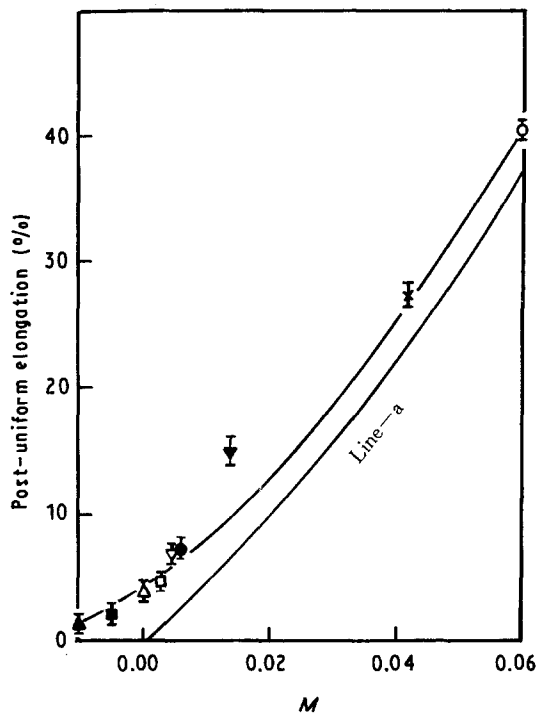

Figure 5 Collected data of Ghosh [17] showing the relation between post-uniform elongation and strain rate sensitivity (M), compared with the theoretical calculation (line-a) with Equation 18. (▼) A-K steel, (●) HSLA steel, (□) C.R. aluminium (1100), (■) 2036-T4 aluminium, (▽) 3003-0 aluminium, (▲) 5182-0 aluminium, (×) 5182-0 aluminium (150 °C), (△) 70–30 brass, (○) Zn–Ti alloy.

References

1. N. C. GOEL, S. SANGAL and K. TANGRI, *Metall. Trans. A* **16** (1985) 2013.
2. S. ANKEM and H. MARGOLIN, *ibid.* **14** (1983) 500.
3. C. KIM, *ibid.* **19** (1988) 1263.
4. K. CHO and J. GURLAND, *ibid.* **19** (1988) 2027.
5. Y. TOMITA and K. OKABAYASHI, *ibid.* **16** (1985) 865.
6. F. H. SAMEL, *Mater. Sci. Engng* **92** (1987) L1.
7. R. D. LAWSON, D. K. MATLOCK and G. KRAUSS, in "Fundamentals of Dual Phase Steel," edited by R. A. Kot and B. L. Bramfitt (TMS-AIME, New York, 1981) p. 437.
8. W. R. CRIBB and J. M. RIGSBEE, in "Structure and Properties of Dual Phase Steels", edited by R. A. Kot and J. W. Morris (TMS-AIME, New York, 1979) p. 91.
9. C. CRUSSARD, *Rev. Metall.* **50** (1953) 697.
10. B. JAOUL, *J. Mech. Phys. Solids* **5** (1957) 95.
11. R. E. REED-HILL, W. R. CRIBB and S. N. MONTEIRO, *Metall. Trans. A* **4** (1973) 2665.
12. F. A. NICHOLS, *Acta Metall.* **28** (1980) 633.
13. J. LIAN, *Chin. J. Mech. Eng.* **18** (4) (1982) 21.
14. J. LIAN and B. BAUDELET, *Mater. Sci. Engng* **84** (1986) 157.
15. S. L. SEMIATIN and J. J. JONAS, "Formability and Workability of Metals" (ASM, Metals Park, Ohio, 1984), p. 155.
16. A. CONSIDERE, *Ann. Ponts. Ch. Ser.* 6 **9** (1885) 574.
17. A. K. GHOSH, *Metall. Trans. A* **8** (1977) 1221.

Received 29 October 1991
and accepted 14 August 1992